

# Surface composition of anhydrous tricalcium aluminate and calcium aluminoferrite

M. C. BALL\*, R. E. SIMMONS\*, I. SUTHERLAND†

\*Department of Chemistry and †Department of Physics, Loughborough University of Technology, Loughborough, Leicestershire LE11 3TU, UK

Electron spectroscopy and optoacoustic spectroscopy (OAS) have been used to study the surfaces of synthetic tricalcium aluminate,  $\text{Ca}_3\text{Al}_2\text{O}_6$  and calcium aluminoferrite,  $\text{Ca}_2\text{AlFeO}_5$ . The surfaces of these compounds have compositions which differ markedly from those of the bulk. The surface of tricalcium aluminate is depleted in calcium and enriched in aluminium and also carries relatively stable hydroxyl groups, which can be detected by OAS. Calcium aluminoferrite has a surface enriched in aluminium and depleted in calcium and iron. Again, some hydroxyl groups are present on the surface. These differences in surface composition are discussed with particular reference to the early stages of reaction with water.

## 1. Introduction

A considerable body of work has been built up over many years concerning the reactions of cement minerals with water [1, 2]. The techniques used have, until recently, been those which determine the properties of bulk phases, e.g. classical chemical analysis, X-ray diffraction and optical and electron microscopy. It follows that the extent of reaction must be relatively high for these techniques to give results. More recently, electron-analytical techniques have reduced the sample size required for analysis [3, 4]. From this work it is apparent that crystallization processes are slow and that there is a great deal of kinetic control of the hydration reactions.

Recently electron spectroscopy (ESCA) has been used to measure the composition of thin films of silicate and aluminate hydrates produced in the very early stages of reaction. The hydration reactions studied in this way have been those of  $\text{C}_3\text{S}^*$  [5-7] and  $\text{C}_2\text{S}$  [8, 9], showing the reduction of calcium concentration in the precipitated layers. Some work has been done to study hydrating  $\text{C}_3\text{A}$  [10, 11]. This work has thrown much light on to the very early stages of reaction, but the surface compositions of the starting materials have been neglected. These are important, in that in the early stages of reaction, part of the ESCA signal comes from the unreacted material, and the unreacted material is usually assumed to have the bulk composition. This assumption is made even though there is increasing evidence that the chemical composition of the surface of many solids is very different from that of the bulk. Most of the work done has been on metals and alloys [12], but some experimental evidence is available for halides and ceramics [13], magnesium oxide especially [14]. All of the work published on magnesium oxide concerns low concentrations of impurity ions, present in solid solution.

This simplification removes the problems which might arise from precipitated secondary phases.

As with most instrumental techniques, problems arise in ESCA of relating the measured signal intensity to element concentration within the sample. The concentration ( $N_A$ ) of atoms of type A is assumed to be related to the peak intensity ( $I_A$ ) by the formula

$$N_A = I_A/S_A$$

where  $S_A$  is the relative sensitivity factor for photoemission from the appropriate orbital on atom A. It is possible, in theory, to calculate the peak intensity for a given photoelectron, and recent publications have listed theoretical sensitivity factors [15]. However, the most straightforward method is to use reference standards [16]. Sensitivity factors are often expressed relative to the oxygen or fluorine 1s orbitals. The concentration ( $C_A$ ) of an element in a sample of unknown composition may then be described:

$$C_A = 100(I_A/S_A)/\Sigma(I_i/S_i)$$

where the sum is over all elements present in the sample surface.

Care must be exercised in the choice of appropriate standards for use in determining sensitivity factors, because, as was mentioned previously, the surface composition of many materials differs from that of the bulk. The difficulty of obtaining a sample with known surface composition limits the accuracy with which relative sensitivity factors may be determined; this limits the absolute accuracy of the surface compositions obtained. In ESCA it is possible to remove an unrepresentative surface layer by ion bombardment to expose bulk material. However, it is not normally advisable to use ion-bombarded materials as standards for the determination of sensitivity factors,

\*Cement nomenclature: C = CaO, A =  $\text{Al}_2\text{O}_3$ , F =  $\text{Fe}_2\text{O}_3$ , S =  $\text{SiO}_2$ .

since recent research has shown that a wide range of inorganic compounds undergo both structural and chemical changes on bombardment [17, 18]. In the present study, relative sensitivity factors for aluminium, calcium, carbon, iron and oxygen were determined from the surfaces of  $\text{Al}_2\text{O}_3$ ,  $\text{Fe}_2\text{O}_3$  and  $\text{CaCO}_3$  powder samples. These materials have proved to be excellent, stable standards over several years. Their sputtering behaviour has been studied [19]. It is possible to ignore the question of sensitivity factors by the use of a range of standards of known bulk composition to derive a calibration curve. This, of course, assumes that the surface composition is the same as the bulk. This calibration method has been used in the few publications so far on the use of ESCA in cement chemistry [5–11].

The present work is a continuation of that carried out on the anhydrous silicates [20] and uses sensitivity factors rather than calibration standards. This reduces assumptions about the surface composition of the materials, while introducing others about the transfer of sensitivity factors between compounds.

## 2. Experimental procedure

### 2.1. Synthesis of compounds

$\text{C}_3\text{A}$  was synthesised from AR calcium carbonate and AR aluminium nitrate by firing at 1650 K.  $\text{C}_4\text{AF}$  was made from the same reagents and Specpure ferric oxide, and fired at 1600 K [21]. Stoichiometric mixtures were fired, ground, and refired several times and the progress of the reactions followed by X-rays. White's test [22] was used to detect free lime. Samples were pressed into discs 13 mm in diameter, at a pressure of 20 ton  $\text{in}^{-2}$  (309 MPa) and refired before examination in the ESCA spectrometer. The samples, when removed from the furnace, were immediately placed in a desiccator over phosphorus pentoxide: the handling time before entering the spectrometer was of the order of 30 sec. A sample of  $\text{C}_3\text{A}$  was also refired at 1750 K for 24 h to attempt to remove hydroxyl groups.

### 2.2. ESCA spectrometer

This was an Escalab 5 Electron Spectrometer manufactured by Vacuum Generators Ltd, Hastings, Sussex, U.K. using either  $\text{AlK}_\alpha$  radiation (1486.6 eV) or  $\text{MgK}_\alpha$  radiation (1254.4 eV). An ion gun using argon was also used to sputter off surface material (3 keV, current density  $12 \mu\text{A cm}^{-2}$ ). About 10 nm of material were removed in the present study, i.e. a thickness approximately equal to that of the analysed layer. Both atomic composition and chemical shifts were measured, the latter by using the carbon peak at 284.7 eV as reference. This was always present due to contamination. The proportion of total carbon present as carbonate was estimated by measurement of the relative peak areas on a high resolution scan.

### 2.3. OAS spectrometer

This was an EDT 400 spectrometer (EDT Research, London), capable of measuring in the UV/visible region (280 to 800 nm) and the near infrared (1.2 to  $3.2 \mu\text{m}$ ). The latter region is very useful for the detec-

TABLE I Surface analyses

Element	Composition (at %)*		
	$\text{C}_3\text{A}(1)$	$\text{C}_3\text{A}(2)$	$\text{C}_4\text{AF}$
<i>Unspattered samples</i>			
Ca	13.5 (27.2)	18.3	13.8 (22.0)
Al	12.9 (18.2)	21.5	9.4 (11.0)
Fe	—	—	3.4 (11.0)
O	57.9 (54.5)	50.1	54.1 (55.0)
S	—	—	2.4
Na	—	—	2.8
Si	—	1.1	—
C	15.7	9.1	14.1
C (as $\text{CO}_3^{2-}$ )	8.4	3.4	4.7
<i>Sputtered samples</i>			
Ca	19.1 (27.2)	—	17.7 (22.0)
Al	25.8 (18.2)	—	17.8 (11.0)
Fe	—	—	5.8 (11.0)
O	55.1 (54.5)	—	58.7 (55.0)

\*Theoretical percentages are in parentheses.  $\text{C}_3\text{A}(1)$  is the original preparation;  $\text{C}_3\text{A}(2)$  is the refired material.

tion of water and hydroxyl groups, since it contains both the overtone and combination bands [23].

## 3. Results

Table I gives the complete surface analyses for the compounds studied, before and after sputtering. The estimates of carbonate are also included. These values are probably accurate to  $\pm 2\%$  in relative terms, with most of this arising from area measurement, and  $\pm 8\%$  in absolute terms. Table II gives the corrected analyses: the correction entails the subtraction of organic carbon, followed by the calcium carbonate equivalent of the inorganic carbon. The sodium and sulphur contents in  $\text{C}_4\text{AF}$  (both of which were present as contaminants, and which were possibly present in the ferric oxide) were treated as oxides, and the silicon in refired  $\text{C}_3\text{A}$  as dicalcium silicate. The composition was then recalculated to 100 at %. The analyses for sputtered samples in Table I do not contain any carbon, so no corrections are necessary, but the values are repeated in Table II. Table II has been converted to atom ratios for Table III. Cation/anion charge ratios have been calculated and are included in Table II. It can be seen from Table III that the surface composition differs from the theoretical for both compounds

TABLE II Corrected surface analyses

Element	Composition (at %)*		
	$\text{C}_3\text{A}(1)$	$\text{C}_3\text{A}(2)$	$\text{C}_4\text{AF}$
<i>Unspattered samples</i>			
Ca	10.0 (27.2)	18.3	15.8 (22.0)
Al	25.4 (18.2)	21.5	17.6 (11.0)
Fe	—	—	6.3 (11.0)
O	64.5 (54.5)	50.1	54.2 (55.0)
+/-	0.75	1.01	0.95
<i>Sputtered samples</i>			
Ca	19.1 (27.2)	—	17.7 (22.0)
Al	25.8 (18.2)	—	17.8 (11.0)
Fe	—	—	5.8 (11.0)
O	55.1 (54.5)	—	58.7 (55.0)
+/-	1.05	—	0.90

\*Theoretical percentages are in parentheses.

TABLE III Atom ratios (corrected data)

Ratio	Compound*		
	C <sub>3</sub> A(1)	C <sub>3</sub> A(2)	C <sub>4</sub> AF
<i>Unspattered samples</i>			
Ca/O	0.16 (0.5)	0.37	0.29 (0.4)
Al/O	0.39 (0.33)	0.43	0.32 (0.2)
Fe/O			0.12 (0.2)
Ca/Al	0.39 (1.5)	0.85	0.90 (2.0)
Ca/Fe			2.51 (2.0)
Al/Fe			2.79 (1.0)
<i>Sputtered samples</i>			
Ca/O	0.35 (0.5)		0.30 (0.4)
Al/O	0.47 (0.33)		0.30 (0.2)
Fe/O			0.10 (0.2)
Ca/Al	0.74 (1.5)		0.99 (2.0)
Ca/Fe			3.05 (2.0)
Al/Fe			3.07 (1.0)

\*Theoretical ratios are in parentheses.

studied. This difference shows itself in a general decrease in calcium and iron contents and an increase in aluminium content. Chemical shift data are given in Table IV. Optoacoustic spectra in the near IR region for the two compounds are shown in Fig. 1. There are strong similarities between the two spectra in the overtone region (0.8 to 1.6  $\mu\text{m}$ ), but the combination region (2.4 to 3.2  $\mu\text{m}$ ) is very different.

## 4. Discussion

### 4.1. Surface composition

#### 4.1.1. Tricalcium aluminate

The ratios in Table III show that the calcium content in the surface layer is lower than theoretical by a factor of 0.37, while the aluminium content is increased by a factor of 1.40, both relative to the bulk concentration. The calculated cation/anion ratio indicates that the protons detected in the OAS spectrum must be contributing to the total cation balance (since the ESCA technique can detect elements down to beryllium). Assuming that this is the case, the analysis suggests a deficiency of 25 protons for 100 other atoms. Recalcu-

TABLE IV Chemical shift data

	Binding energy (eV)*		
	C <sub>3</sub> A(1)	C <sub>3</sub> A(2)	C <sub>4</sub> AF
Ca 2p	346.6	346.2	345.9
Al 2p	73.0	71.9	72.6
Fe 2p			710.4
O 1s	531.0	{ 529.0 530.2	{ 529.1 531.2

\*Shifts are relative to C 1s = 284.7 eV.

lation on this basis gives the composition Ca 7.9%, Al 20.2%, H 20.3%, O 51.4%. This is equivalent to a stoichiometric formula of  $\text{CaAl}_{2.5}\text{O}_4(\text{OH})_{2.5}$ .

These values are averaged over a layer more than 5.0 nm thick and therefore the outer layers must be more hydroxylated (and richer in aluminium) than the average. This suggests that a considerable proportion of the surface oxygens must be fully protonated and hence the composition of the extreme outer layers must approach that of aluminium hydroxide. In support of these suggestions, the OAS spectrum shown in Fig. 1 indicates that C<sub>3</sub>A shows absorption in the Al-OH overtone region (0.8 to 1.6  $\mu\text{m}$ ) [23].

Room-temperature sorption of water may account for this spectrum, but it is unlikely to cause subsequent ion movements to give the observed element concentrations. This suggests that the hydroxyl groups are still present at the firing temperature, when ion diffusion can accommodate the different charge balance. This indicates that the hydroxyl groups are extremely stable: calculations on the stability of hydroxyl groups in magnesium oxide agree with this (see [24] and references therein). The sputtered material gives an analysis which is closer to the theoretical values, but which still shows increased aluminium levels and lowered calcium levels. In this case the calculated cation/anion ratio is very close to unity, indicating that the proton-containing layer has been removed by ion bombardment. It is therefore likely that this layer is less than 10 nm thick. The surface is considerably

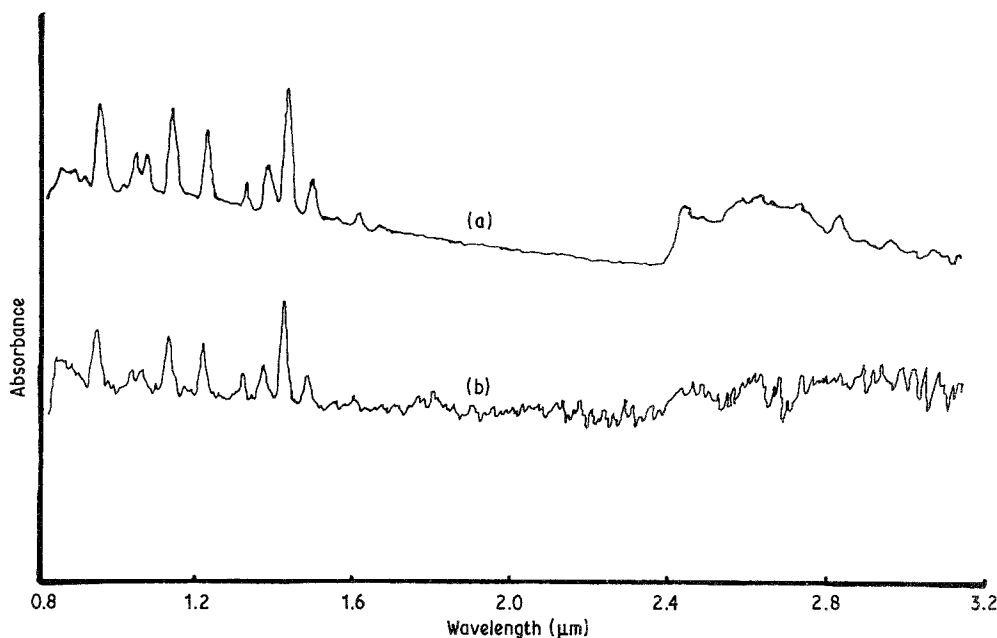


Figure 1 Optoacoustic spectra for tricalcium aluminate and calcium aluminoferrite: (a) C<sub>3</sub>A (sensitivity 1 mV); (b) C<sub>4</sub>AF (sensitivity 0.1 mV).

enriched in oxygen. It is possible that this is caused by an outward movement of oxide ions and a complementary inward movement of cations, as has been suggested for alkali halides [25]. The sputtered material has the correct oxygen concentration, within experimental error.

#### 4.1.2. Refired tricalcium aluminate

Table III suggests that long firing increases both calcium and aluminium levels in the surface, although the theoretical values are not reached. In this case the cation/anion ratio is very close to unity, indicating that the protons can be removed on very long heating. However, enrichment by aluminium still takes place.

#### 4.1.3. Calcium ferrite

The surface of the ferrite phase is enriched in aluminium by a factor of 1.60 and depleted in calcium by a factor of 0.72 while the iron concentration is reduced by a factor of 0.57. The calculated cation/anion ratio is less than unity and again, hydroxyl absorption can be seen in the OAS spectrum (Fig. 1). Sputtering of the surface increases the concentration of all the elements present, but has a greater effect on the calcium and iron contents. The cation/anion ratio is made worse by sputtering, because some of the Fe(III) is apparently reduced to Fe(II), as discussed in the next section.

### 4.2. Chemical shift results [5]

#### 4.2.1. Oxygen

The oxygen peak in  $C_3A$  is broad and shows asymmetry to the low binding energy side. Refiring splits the peak towards low binding energies, indicating two components of approximately equal intensity. This suggests that there are two types of oxygen produced on heating, and that these are rather more negative than in the original preparation. The crystal structure shows that there are both terminal and bridging oxygens present [26], and if protons were removed on refiring, this would account for the observed shifts.

Similar asymmetric splitting of the oxygen peak is observed for  $C_4AF$ . On refiring, the splitting is increased and the peaks become roughly equal in intensity.

#### 4.2.2. Calcium

The peak energy for  $C_3A$  is similar to that of calcium oxide, while the value for  $C_4AF$  is lower. This peak is also broadened, suggesting at least two sites for calcium.

#### 4.2.3. Aluminium

A reduction in binding energy of 1 eV is observed for the Al  $2p$  electrons on refiring. This perhaps agrees with the oxygen results, in that removal of protons will allow a general redistribution of charge across the  $AlO_4$  tetrahedra.

#### 4.2.4. Iron

The binding energy of 710.4 eV in  $C_4AF$  is rather low. The peak is single in the unsputtered material, indicating that there is no range of sites available. In the sputtered material, the peak is sharper and a slight

shoulder appears on the low binding energy side, probably resulting from ion-induced decomposition. No other evidence could be found, in any of the components studied, for ion decomposition.

A considerable amount of work has been done on the segregation of impurity ions in inorganic oxide and halide systems [12, 13] as well as in metals [10]. Although the ion movements discussed here are by no means those of impurities, the processes are sufficiently similar to merit consideration. Unfortunately, the range of variables leading to segregation is very wide, and it is not possible to arrive at any single driving force. Since, for example, in the ferrite, aluminium is enriched at the surface and iron is depleted, it is clear that more than charge is involved in the redistribution. Attempts to relate the enrichments to various charge/size parameters were unsuccessful.

### 4.3. Reaction with water

#### 4.3.1. Tricalcium aluminate

The literature on the hydration of  $C_3A$  is extensive. Glasser and Marhino, in a recent paper [27], have summarized the work on the early stages of reaction of  $C_3A$  and its sodium-containing solid solutions. On contact with water, an incongruent solution process occurs, with calcium entering the solution preferentially. It is therefore suggested that this leaves an alumina-rich layer on the surface of the solid within the first few seconds of reaction. Longer reaction times lead to the precipitation of hydrated calcium aluminates. The results presented here indicate that an alumina-rich layer is present at the surface at the start of the reaction, and is not solely the consequence of incongruent dissolution, although this process obviously becomes increasingly important with time of reaction. This alumina-rich layer may well be kinetically stabilized and act as a template for the precipitation of secondary phases during the early stages of the hydration. Glasser and Marhino suggest that the alumina-rich layer is up to  $1\ \mu\text{m}$  thick in the very early stages of hydration, and  $5\ \mu\text{m}$  when precipitation of the hydrate phases takes place. These calculations are based on the amount of material in solution and the dimensions of the reacting particles. These thicknesses are much greater than that of the original surface layer.

#### 4.3.2. Calcium ferrite

Little work has been done on the very early stages of the reaction between the ferrite phase and water. Most published work argues that there are strong analogies with tricalcium aluminate [28, 29]. This, together with the results from the various silicates studied [20] would suggest that an alumina-rich layer should be formed in this hydration also.

### Acknowledgement

We wish to thank the British Technology Group for their generous support of this programme.

### References

1. H. F. W. TAYLOR, "The Chemistry of Cements" (Academic, London 1964).

2. F. M. LEA, "The Chemistry of Cement and Concrete" (Arnold, London, 1970).
3. H. F. W. TAYLOR and D. E. NEWBURY, *Cem. Concr. Res.* **14** (1984) 93.
4. *Idem, ibid.* **14** (1984).
5. D. MENETRIER, I. JAWED, T. S. SUN and J. SKALNY, *ibid.* **9** (1979) 473.
6. *Idem, ibid.* **10** (1980) 425.
7. *Idem, ibid.* **11** (1981) 297.
8. J. -H. THOMASSIN, M. REGOURD, P. BAILLIF and J. -C. TOURAY, *C. R. Acad. Sci. (C)* **288** (1979) 93.
9. M. REGOURD, J. -H. THOMASSIN, P. BAILLIF and J. -C. TOURAY, in Proceedings of 7th International Congress on the Chemistry of Cement, Vol. 2 (Septima, Paris, 1980) p. II-123.
10. M. E. TADROS, W. Y. JACKSON and J. SKALNY, in Proceedings of International Conference on Colloids and Surfaces, Puerto Rico, 1976, Vol. IV, edited by M. Kerker, p. 211.
11. I. JAWED and J. SKALNY, in Proceedings of International Seminar on Calcium Aluminates, Torino, 1982.
12. E. D. HONDROS and M. P. SEAH, *Int. Met. Rev.* **262** (December 1977).
13. W. D. KINGERY, *J. Amer. Ceram. Soc.* **57** (1974) 74.
14. E. A. COLBOURN and W. C. MACKRODT, *J. Mater. Sci.* **17** (1982) 3021.
15. J. SZAJMAN, J. C. JENKIN, R. C. G. LECKAY and J. LIESEGANG, *J. Electr. Spectr. Rel. Phenom.* **19** (1980) 393.
16. D. BRIGGS, "Handbook of X-Ray and Ultraviolet Photoelectron Spectroscopy" (Heyden, London, 1977).
17. R. KELLY, *Surf. Sci.* **90** (1979) 280.
18. *Idem, ibid.* **100** (1980) 85.
19. R. KELLY and N. G. LAM, *Radiat. Eff.* **19** (1973) 39.
20. M. C. BALL, R. E. SIMMONS and I. SUTHERLAND, *Brit. Ceram. Proc.* **35** (1985) 1.
21. F. M. LEA, "The Chemistry of Cement and Concrete" (Arnold, London, 1970) pp. 49, 57.
22. *Idem, ibid.* p. 108.
23. R. F. GODDU, *Adv. Anal. Chem. Instrum.* **1** (1960) 347.
24. T. H. NEILSON and M. H. LEOPOLD, *J. Amer. Ceram. Soc.* **49** (1966) 626.
25. G. C. BENSON, P. I. FREEMAN and E. DEMPSEY, *Adv. Chem. Ser.* **33** (1961) 26.
26. P. MONDAL and J. W. JEFFERY, *Acta Crystallogr.* **B31** (1975) 689.
27. F. P. GLASSER and M. B. MARINHO, *Br. Ceram. Proc.* **35** (1985) 221.
28. I. JAWED, S. GOTO and R. KONDO, *Cem. Concr. Res.* **6** (1976) 441.
29. C. PLOWMAN and J. G. CABRERA, *ibid.* **14** (1984) 238.

*Received 17 June  
and accepted 11 November 1986*